Advances in Nano Research, *Vol. 12, No. 4 (2022) 353-363*
https://doi.org/10.12989/anr.2022.12.4.353

Superharmonic and subharmonic resonances of a carbon nanotube-reinforced composite beam

M. Alimoradzadeh[1] and Ş.D. Akbaş*[2]

[1]*Department of Mechanical Engineering, Najafabad Branch, Islamic Azad University, Najafabad, Iran*
[2]*Department of Civil Engineering, Bursa Technical University, 16330, Bursa, Turkey*

(*Received September 12, 2021, Revised December 31, 2021, Accepted January 4, 2022*)

Abstract. This paper presents an investigation about superharmonic and subharmonic resonances of a carbon nanotube reinforced composite beam subjected to lateral harmonic load with damping effect based on the modified couple stress theory. As reinforcing phase, three different types of single walled carbon nanotubes (CNTs) distribution are considered through the thickness in polymeric matrix. The governing nonlinear dynamic equation is derived based on the von Kármán nonlinearity with using of Hamilton's principle. The Galerkin's decomposition technique is utilized to discretize the governing nonlinear partial differential equation to nonlinear ordinary differential equation and then is solved by using of multiple time scale method. Effects of different patterns of reinforcement, volume fraction, excitation force and the length scale parameter on the frequency-response curves of the carbon nanotube reinforced composite beam are investigated. The results show that volume fraction and the distribution of CNTs play an important role on superharmonic and subharmonic resonances of the carbon nanotube reinforced composite beams.

Keywords: carbon nanotubes; composites; couple stress theory; nonlinear vibration; superharmonic and subharmonic resonances

1. Introduction

Carbon nanotubes (CNTs) are a kind of reinforcements whose properties includes strength-to-weight. CNTs are discovered by Sumio Iijima (1991) and using CNTs in many applicants has increasing day by day such as medicine, electronic devices, composites (Ruoff and Lorents 1995, Salvetat *et al*. 1999, Li *et al*. 2002, Yakobson and Avouris 2001, Mamidi *et al*. 2017, 2019, 2021, Zavala *et al*. 2021).

Due to its flexible properties, CNTs behave large deflections and so the mechanical behavior of CNTs and its structures must be studied using nonlinear analysis. In last decade, many studies have been performed on the dynamic and static and stability of composite beams reinforced by CNTs. Some investigations about the dynamic and static and stability analyses of CNTs reinforced beams are summarized as following. Shen (2009) investigated nonlinear static analysis of functionally graded nano-composite plates reinforced by SWCNTs under thermal effect. Ke *et al*. (2010) investigated nonlinear vibration functionally graded nanobeams reinforced by CNTs by using Timoshenko beam theory and von Kármán geometric nonlinearity. Yas and Samadi (2012) investigated vibration and stability of CNT nanocomposite beams resting on elastic foundation by using differential quadrature method. Wattanasakulpong and Ungbhakorn (2013) analyzed buckling, static and dynamics of CNT reinforced beams resting on elastic foundation by Navier solution. Rafiee *et al*. (2014) studied non-linear dynamic stability of piezoelectric CNT reinforced composite plates. Akbaş (2016b, c, 2017a, b, 2018c) analyzed vibration and static analysis of homogeneous and composite nano structures. Fernandes *et al*. (2016) presented nonlinear dynamic responses of microbeams by using finite strain and velocity gradient theories. Shi *et al*. (2017) presented free vibration of functionally graded CNTs beams with different boundary conditions. Tornabene *et al*. (2017) investigated vibration analysis of CNT/polymer/fiber laminated nanocomposite structures by using generalized differential quadrature method. Tagrara *et al*. (2015) solved static, free vibration and buckling analysis of CNTs composite beams embedded in elastic foundation by using high order beam theory. Thang *et al*. (2017) studied nonlinear buckling of functionally graded CNTs plates by analytically. Ghayesh (2009, 2012), Ghayesh *et al*. (2012a, b) investigated nonlinear vibration and stability analysis of beams resting on elastic foundation. Heidari and Arvin (2019) analyzed nonlinear free vibrations of functionally graded rotating beams reinforced by CNT by using Timoshenko beam theory and Von-Karman nonlinearity. Ebrahimi and Dabbagh (2018a, b, c) investigated wave propagation nano scale different composite structures. Fernandes *et al*. (2016) presented nonlinear dynamic responses of microbeams by using finite strain and velocity gradient theories. Alimoradzadeh *et al*. (2019, 2020) investigated nonlinear dynamic responses of homogeneous and inhomogenous beams resting on nonlinear elastic foundation. Akbaş (2016a, 2017c), Kocatürk and Akbaş (2013) investigated forced vibration responses of a viscoelastic nanobeams by using finite element method.

*Corresponding author, Ph.D.,
E-mail: seref.akbas@btu.edu.tr; serefda@yahoo.com

ISSN: 2287-237X (Print), 2287-2388 (Online)

Akbaş (2018a, b, 2019a, b) analyzed the effects of cracks on the forced vibration responses of nano beams and rods. Ebrahimi *et al*. (2016) presented vibration and buckling results of nanotube under thermal effect based on Eringen's nonlocal elasticity theory by using differential transformation method. Chu *et al*. (2020) presented a review study about nonlinear absorption properties of carbon nanotubes. Guo and Zhang (2016) investigated nonlinear vibration of a composite plate reinforced by CNTs subjected to combined forceds by using the Galerkin method. Wu *et al*. (2018) investigated nonlinear free vibration of multi-walled CNTs resting on foundation. Alimoradzadeh and Akbaş (2021a, b) presented superharmonic and subharmonic resonances of cracked atomic force microscopes based on the modified couple stress theory. Babu Arumugam *et al*. (2019) obtained finite element solution of dynamic responses of CNTRC beams. Ponnusami *et al*. (2020) examined nonlinear static nad stability of CNTs by using variational asymptotic method. Ton-That (2020) examined nonlinear free vibrations functionally graded CNTs plates by using Four-Node Quadrilateral Element. Civalek *et al*. (2021a, b) investigated free and forced vibration of carbon nanotube-reinforced composite microbeams. Van Do (2020) investigated free vibration and dynamic transient responses of CNT reinforced plates by using Bézier extraction based isogeometric analysis method coupled and higher-order shear deformation theory. Ghayesh (2019) investigated nonlinear dynamic responses of functionally graded composite beams with viscoelastic model. Ghayesh (2018a, b, Bousahla *et al*. 2020) presented stability and vibration analysis of beams by reinforced CNTs resting on Winkler-Pasternak elastic foundation by using the Navier solution. Al-Furjan *et al*. (2020) analyzed wave propagation of a sandwich doubly curved nanocomposite panel. Huang *et al*. (2021) investigated buckling of micro shell panels by reinforced CNTs. Kumar *et al*. (2021) investigated nonlocal vibration analysis of graded nanostructures with porosity.

In the literature, superharmonic and subharmonic resonances of composite beams by reinforced carbon nanotubes (CNTRC) has not been investigated broadly. Main goal of presented paper is to investigate superharmonic and subharmonic resonances of CNT reinforced composite under lateral harmonic load with damping effect based on the modified couple stress theory by using Galerkin's decomposition technique with using of multiple time scale method. Effects of patterns of reinforcement, volume fraction, excitation force and the length scale parameter on the frequency-response curves and phase trajectory of the carbon nanotube reinforced composite beam are investigated.

2. Problem formulation

A straight simply supported CNT reinforced composite beam of length L, thickness h and width b, in x, y and z direction is considered as shown in Fig. 1. It is assumed that the simply supported beam is subjected to supersonic air flow. In this study, three different patterns of CNTs reinforcement over the beam are considered as uniform

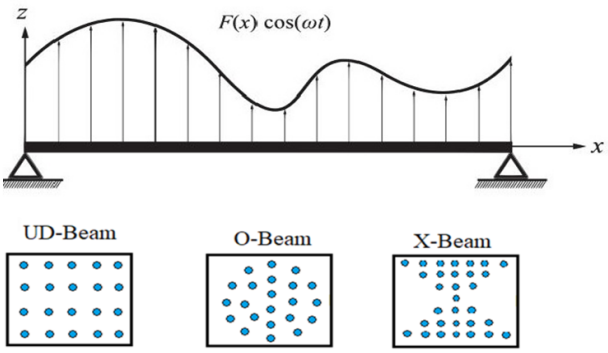

Fig. 1 CNTRC simply supported beam under to lateral distributed harmonic excitation load with three different patterns of CNTs

distribution (UD), and functionally distribution O and X as shown in Fig. 1.

It is assumed that, the CNTs are embedded in an isotropic polymer matrix without abrupt interface through whole region of the beam. In order to represents the effective material properties of carbon nanotube-reinforced composite (CNTRC), the rule of mixture model can be used. Based on the rule of mixture model, modulus of Young's modulus E, shear modulus G, Poisson's ratio ϑ and density ρ of the CNTRC beams can be defined as below (Wattanasakulpong and Ungbhakorn 2013, Shen 2009)

$$E_{11} = \eta_1 V_{CNT} E_{11}^{CNT} + V_p E^p \tag{1}$$

$$\frac{\eta_2}{E_{22}} = \frac{V_{CNT}}{E_{22}^{CNT}} + \frac{V_p}{E^p} \tag{2}$$

$$\frac{\eta_3}{G_{12}} = \frac{V_{CNT}}{G_{12}^{CNT}} + \frac{V_p}{G^p} \tag{3}$$

$$V_{CNT} + V_p = 1 \tag{4}$$

$$v = V_{CNT} v^{CNT} + V_p v^p \tag{5}$$

$$\rho = V_{CNT} \rho^{CNT} + V_p \rho^p \tag{6}$$

where superscripts *CNT* and p symbolize the related material properties of carbon nanotube and polymer matrix, respectively. η_1, η_2, η_3 can be indicated the efficiency parameters of CNT. Also, V_{CNT} and V_p define the volume fractions for CNT and polymer matrix, respectively. Volume fractions of CNTs as a function of thickness direction for different patterns of CNTs (Wattanasakulpong and Ungbhakorn 2013) are presented in Table 1. In this table, V_{CNT}^* is the given volume fraction of CNTs. In this study, the efficiency parameters of CNTs for three different values of V_{CNT}^* are considered as (Yas and Samadi 2012);

$$\eta_1 = 1.2833, \eta_2 = \eta_3 = 1.055 \quad \text{for} \quad V_{CNT}^* = 0.12 \tag{7a}$$

$$\eta_1 = 1.3414, \eta_2 = \eta_3 = 1.7101 \quad \text{for} \quad V_{CNT}^* = 0.17 \tag{7b}$$

$$\eta_1 = 1.3238, \eta_2 = \eta_3 = 1.738 \quad \text{for} \quad V_{CNT}^* = 0.28 \tag{7c}$$

Table 1 For different distributions of CNTs Volume fractions of CNTs dependent thickness direction (Wattanasakulpong and Ungbhakorn 2013)

Patterns of CNTs	V_{CNT}
UD	V_{CNT}^{*}
O	$2V_{CNT}^{*}\left(1-2\frac{\lvert z\rvert}{h}\right)$
X	$4V_{CNT}^{*}\frac{\lvert z\rvert}{h}$

The normal stress and nonlinear strain-displacement component relationship can be defined by using of Von-Karman strain nonlinearity as follows;

$$\sigma_{xx}=\frac{E_{11}(z)}{1-\vartheta^{2}(z)}\varepsilon_{xx} \tag{8a}$$

$$\varepsilon_{xx}=\frac{\partial u}{\partial x}-z\frac{\partial^{2}w}{\partial x^{2}}+\frac{1}{2}\left(\frac{\partial w}{\partial x}\right)^{2} \tag{8b}$$

where u and w represent axial and lateral displacement of the midplane along x and z direction, respectively.

Based on the modified couple stress theory, the strain energy of the beam is given as follows:

$$U=\frac{1}{2}\int_{v}\left(\sigma_{ij}\varepsilon_{ij}+m_{ij}\chi_{ij}\right)dV \quad i,j,k\in[x,y,z] \tag{9}$$

where, ε_{ij} and $\boldsymbol{\chi_{ij}}$ denote the components of the strain tensor and the symmetric part of the curvature tensor, respectively. Also in Eq. (1) σ_{ij} and m_{ij} denotes the stress tensor and the deviatoric part of couple stress tensor respectively and can be define as below

$$\sigma_{ij}=\lambda\varepsilon_{kk}\delta_{ij}+2\mu\varepsilon_{ij} \tag{10a}$$

$$m_{ij}=2\mu\mathbf{l}^{2}x_{ij} \tag{10b}$$

$$\chi_{ij}=\frac{1}{2}\left(\frac{\partial\theta_{i}}{\partial x_{j}}+\frac{\partial\theta_{j}}{\partial x_{i}}\right) \tag{10c}$$

where, $\mathbf{l}$ is the material length scale parameter δ_{ij} is the Kronecker delta, and θ is the rotation vector, $\boldsymbol{\lambda}$ and μ are lame's constants that can be expressed as below

$$\lambda=\frac{\boldsymbol{E\,\vartheta}}{(\mathbf{1}+\boldsymbol{\vartheta})(\mathbf{1}-\mathbf{2}\boldsymbol{\vartheta})} \tag{11a}$$

$$\mu=\frac{\mathbf{E}}{2(1+\boldsymbol{\vartheta})} \tag{11b}$$

$$\theta_{x}=\theta_{z}=0\ ,\ \theta_{y}=-\frac{\partial w}{\partial x} \tag{11c}$$

Using of Eqs. (10) and (11) leads to the non-zero components of the symmetric curvature tensor and the couple stress tensor as follows:

$$\chi_{xy}=\chi_{yx}=-\frac{1}{2}\frac{\partial^{2}w}{\partial x^{2}} \tag{12a}$$

$$m_{xy}=m_{yx}=-\mu l^{2}\frac{\partial^{2}w}{\partial x^{2}} \tag{12b}$$

Substituting Eqs. (8) and (10)-(12), into Eq. (9) leads to

$$U_{s}=\frac{1}{2}\int_{0}^{L}\begin{bmatrix}A_{11}\left(\frac{\partial u}{\partial x}+\frac{1}{2}\left(\frac{\partial w}{\partial x}\right)^{2}\right)^{2}\\-2B_{11}\frac{\partial^{2}w}{\partial x^{2}}\left(\frac{\partial u}{\partial x}+\frac{1}{2}\left(\frac{\partial w}{\partial x}\right)^{2}\right)\\+(D_{11}+\Gamma)\left(\frac{\partial^{2}w}{\partial x^{2}}\right)^{2}\end{bmatrix}dx \tag{13}$$

where

$$A_{11},B_{11},D_{11}=\int_{A}\frac{E_{11}(z)}{1-\vartheta^{2}(z)}(1,z,z^{2})dA \tag{14a}$$

$$\int_{A}G(z)l^{2}dA=\Gamma \tag{14b}$$

The CNT reinforced composite beam is subjected to external forces includes lateral harmonic force and damping force due to medium. The virtual work done by external forces and the kinetic energy of the beam can be defined as follows:

$$W^{EXT}=\int_{0}^{L}[(F_{D}+F_{w})w(x,t)]dx \tag{15}$$

where

$$F_{D}=-C_{d}\frac{\partial w}{\partial t} \tag{16a}$$

$$F_{w}=F(x)\cos(\Omega t) \tag{16b}$$

In above equations $F(x)$ and Ω represents transverse external load and the frequency of the excitation force respectively. Also, is the coefficient of the viscous damping due to viscous medium.

The kinetic energy (K) of the beam can be expressed as below

$$K=\frac{1}{2}\int_{0}^{L}\left\{I_{0}\left[\left(\frac{\partial u}{\partial t}\right)^{2}+\left(\frac{\partial w}{\partial t}\right)^{2}\right]+I_{2}\left(\frac{\partial^{2}w}{\partial x\,\partial t}\right)-2I_{1}\left(\frac{\partial u}{\partial t}\frac{\partial^{2}w}{\partial x\,\partial t}\right)\right\}dx^{2} \tag{17}$$

where

$$I_{0},I_{1},I_{2}=\int_{A}\rho(z)(1,z,z^{2})dA \tag{18}$$

where ρ indicates the mass density. The nonlinear partial differential equation governing the motion can be derived by using of Hamilton's principle which is expressed as below

$$\delta\int_{t_{1}}^{t_{2}}[K-U_{s}+W^{EXT}]dt=0 \tag{18}$$

where δ denotes the variational symbol. Substituting Eqs. (13), (15), (16) and (17) into Eq. (19) leads to nonlinear governing equation of the CNT composite beams of the CNT composite beams as follows:

$$\frac{\partial}{\partial x}\left[A_{11}\left(\frac{\partial u}{\partial x}+\frac{1}{2}\left(\frac{\partial w}{\partial x}\right)^{2}\right)-B_{11}\frac{\partial^{2}w}{\partial x^{2}}\right]=I_{0}\frac{\partial^{2}u}{\partial t^{2}}-I_{1}\frac{\partial^{3}w}{\partial x\,\partial t^{2}} \tag{20}$$

$$\begin{aligned}&I_0\frac{\partial^2 w}{\partial t^2}+\frac{\partial}{\partial x}\left[I_1\frac{\partial^2 u}{\partial t^2}-I_2\frac{\partial^3 w}{\partial x\,\partial t^2}\right]\\&+C_d\frac{\partial w}{\partial t}++\frac{\partial^2}{\partial x^2}\left[(D_{11}+\Gamma)\frac{\partial^2 w}{\partial x^2}-B_{11}\left(\frac{\partial u}{\partial x}+\frac{1}{2}\left(\frac{\partial w}{\partial x}\right)^2\right)\right]\\&-\frac{\partial}{\partial x}\left[A_{11}\left(\frac{\partial u}{\partial x}+\frac{1}{2}\left(\frac{\partial w}{\partial x}\right)^2\right)-B_{11}\frac{\partial^2 w}{\partial x^2}\right]\frac{\partial w}{\partial x}\\&-\left[A_{11}\left(\frac{\partial u}{\partial x}+\frac{1}{2}\left(\frac{\partial w}{\partial x}\right)^2\right)-B_{11}\frac{\partial^2 w}{\partial x^2}\right]\frac{\partial^2 w}{\partial x^2}=F_0\cos(\Omega t)\end{aligned}\tag{21}$$

In the case of Euler-Bernoulli beam theory, the axial inertia and the rotational inertia of the beam cross section can be neglected. By ignoring the axial inertia, the rotational inertia and the external force due free oscillation analysis the Eqs. (20) and (21) takes the following form:

$$\frac{\partial}{\partial x}\left[A_{11}\left(\frac{\partial u}{\partial x}+\frac{1}{2}\left(\frac{\partial w}{\partial x}\right)^2\right)-B_{11}\frac{\partial^2 w}{\partial x^2}\right]=0\tag{22}$$

Eq. (22) can be reformulated as below:

$$\frac{\partial^2 u}{\partial x^2}=\frac{\partial}{\partial x}\left[-\frac{1}{2}\left(\frac{\partial w}{\partial x}\right)^2+\frac{B_{11}}{A_{11}}\frac{\partial^2 w}{\partial x^2}\right]\tag{23}$$

Integrating Eq. (23) along x-axis yields:

$$\frac{\partial u}{\partial x}=-\frac{1}{2}\left(\frac{\partial w}{\partial x}\right)^2+\frac{B_{11}}{A_{11}}\frac{\partial^2 w}{\partial x^2}-\frac{N_0(t)}{A_{11}}\tag{24}$$

The integration of Eq. (24) leads to:

$$u=\int_0^x-\frac{1}{2}\left(\frac{\partial w}{\partial x}\right)^2dx+\frac{B_{11}}{A_{11}}\frac{\partial w}{\partial x}-\frac{N_0 x}{A_{11}}+N_1(t)\tag{25}$$

It is assumed that the beam has immovable support. Hence, the following boundary condition can be considered:

$$u(0,t)=u(L,t)=0\tag{26}$$

Substituting Eq. (26) into Eq. (25) yields

$$N_0=-\frac{A_{11}}{2L}\int_0^L\left(\frac{\partial w}{\partial x}\right)^2dx+\frac{B_{11}}{L}\left[\frac{\partial w(L,t)}{\partial x}-\frac{\partial w(0,t)}{\partial x}\right]\tag{27}$$

$$N_1(t)=-\frac{B_{11}}{A_{11}}\frac{\partial w(0,t)}{\partial x}\tag{28}$$

Finally, by substituting Eqs. (22) and (24) into Eq. (21), one can obtain the following nonlinear partial differential equation governing the forced vibration of the CNT composite beam:

$$\begin{aligned}&I_0\frac{\partial^2 w}{\partial t^2}+C_d\frac{\partial w}{\partial t}+\left[\left(D_{11}-\frac{B_{11}{}^2}{A_{11}}\right)+\Gamma\right]\frac{\partial^4 w}{\partial x^4}+N_0\frac{\partial^2 w}{\partial x^2}\\&=F(x)\cos(\Omega t)\end{aligned}\tag{29}$$

where $N_0(t)$ is expressed in Eq. (27). In order to derive the governing ordinary differential equation of motion from the partial one mentioned in Eq. (29), the Galerkin's method, is utilized. Based on the Galerkin's method, the solution of the governing equation can be defined as below:

$$\hat{w}(x,t)=\sum_{n=1}^{\infty}\psi_n(x)\,.\,q_n(t)\tag{30}$$

where $\psi_n(x)$ and $q_n(t)$ are the n-th mode shape function (admissible function) and n-th is the modal coefficient respectively. Since the dominant mode in the beam is the first mode, the solution of Eq. (29) can be express as follows:

$$w(x,t)=\psi(x).q(t)\tag{31}$$

For the simply supported beam boundary conditions without axial movement at both ends the mode shape function can be express as follows (Şimşek 2014)

$$\psi(x)=\sin\left(\frac{\pi x}{L}\right)\tag{32}$$

where satisfies the following kinematic boundary conditions for simply supported beam (Ansari *et al*. 2010)

$$w(0,t)=\frac{\partial^2 w(0,t)}{\partial x^2}=0\tag{33}$$

$$w(L,t)=\frac{\partial^2 w(L,t)}{\partial x^2}=0\tag{34}$$

Substituting Eq. (32) in to Eq. (29) leads to:

$$\ddot{q}[I_0\psi]+C_d\psi\dot{q}+a_1q+a_2q^2+a_3q^3=F_0\cos(\Omega t)\tag{35}$$

where $\ddot{q}(t)$ is the second derivative of q(t) with respect to time. Also, the coefficientsa_0, a_1 , a_2 and a_3 are:

$$\begin{aligned}a_1&=\psi_{xxxx}\left[\left(D_{11}-\frac{B_{11}{}^2}{A_{11}}\right)+\Gamma\right],\\a_2&=\frac{B_{11}}{L}\psi_{xx}[\psi_x(L)-\psi_x(0)],\\a_3&=\psi_{xx}\left[-\frac{A_{11}}{2L}\int_0^L{\psi_x}^2dx\right]\end{aligned}\tag{36}$$

where ψ_x, ψ_{xx} and ψ_{xxxx}, respectively, are the first, the second, and the fourth derivative of $\psi(x)$ with respect to x.

Considering the transverse external load as $F(x)=f_0.\psi(x)$, multiplying both side of Eq. (35) with a mode shape function $\psi(x)$ and integrating the result equation over domain (0,L) leads to the nonlinear ordinary differential equation governing the motion of the microscale CNTR composite beam as follows:

$$\ddot{q}+2\hat{\mu}\dot{q}+\omega_0^2q+\hat{\eta}_2q^2+\hat{\eta}_3q^3=f\cos(\Omega t)\tag{37}$$

where

$$\hat{\mu}=\frac{1}{2}\left(\frac{\int_0^L C_d\psi^2dx}{\int_0^L I_0\psi^2(x)dx}\right)\tag{38a}$$

$$\omega_0^2=\frac{\int_0^L a_1\psi(x)dx}{\int_0^L I_0\psi^2(x)dx}\tag{38b}$$

$$\hat{\eta}_2=\frac{\int_0^L a_2\psi(x)dx}{\int_0^L I_0\psi^2(x)dx}\tag{38c}$$

$$\hat{\eta}_3=\frac{\int_0^L a_3\psi(x)dx}{\int_0^L I_0\psi^2(x)dx}\tag{38d}$$

$$\mathrm{f}=\frac{\int_0^{\mathrm{L}} f_0.\psi^2(x)\mathrm{dx}}{\int_0^{\mathrm{L}} \mathrm{I}_0\psi^2(\mathrm{x})\mathrm{dx}} \tag{38e}$$

where, f_0 is the amplitude of the lateral external load. The nonlinear ordinary differential equation is solved by using the method of multiple scales. In order to obtain solution assumption, following assumption is used.

$$\hat{\mu}=\epsilon\mu \tag{39a}$$

$$\hat{\eta}_2=\epsilon\eta_2 \tag{39b}$$

$$\hat{\eta}_3=\epsilon\eta_3 \tag{39c}$$

ϵ indicates bookkeeping parameter. Inserting Eq. (39) to Eq. (37) yields

$$\ddot{\mathrm{q}}+2\epsilon\mu\dot{\mathrm{q}}+\omega_0^2\mathrm{q}+\epsilon\eta_2\mathrm{q}^2+\epsilon\eta_3\mathrm{q}^3=f\cos(\Omega t) \tag{40}$$

In method of multiple scales, time variable is defined as following

$$\mathrm{T_n}=\epsilon^{\mathrm{n}}\mathrm{t}\,,\mathrm{n}=0,1,2,3,.. \tag{41}$$

With processing chain rule for Eq. (39), the following form is obtained:

$$\frac{\mathrm{d}}{\mathrm{dt}}=\mathrm{D}_0+\epsilon\mathrm{D}_1+\epsilon^2\mathrm{D}_2+\epsilon^3\mathrm{D}_3+\cdots \tag{42a}$$

$$\begin{aligned}\frac{\mathrm{d}^2}{\mathrm{dt}^2}=\mathrm{D}_0^2+2\theta\mathrm{D}_0\mathrm{D}_1+\theta^2(\mathrm{D}_1^2+2\mathrm{D}_0\mathrm{D}_2)\\+2\theta^3(\mathrm{D}_1\mathrm{D}_2)+\cdots\end{aligned} \tag{42b}$$

where

$$\mathrm{D_i}=\frac{\partial}{\partial\mathrm{T_i}},\quad \mathrm{i}=0,1,2,3 \tag{43}$$

Solution of Eq. (40) in method of multiple scales obtained as follows (Nayfeh *et al*. 1980, Shafiei and Setoodeh 2017)

$$\mathrm{q}(\mathrm{t},\epsilon)=\mathrm{q}_0(\mathrm{T}_0,\mathrm{T}_1)+\epsilon\mathrm{q}_1(\mathrm{T}_0,\mathrm{T}_1)+\epsilon^2\mathrm{q}_2(\mathrm{T}_0,\mathrm{T}_1) \tag{44}$$

Substituting Eq. (44) into Eq. (40) together with using Eqs. (42) and then equating coefficient of similar power of ϵ to zero yields

$$(\mathrm{D}_0^2+\omega_0^2)\mathrm{q}_0=f\cos(\Omega t) \tag{45}$$

$$(\mathrm{D}_0^2+\omega_0^2)\mathrm{q}_1=-2\mathrm{D}_0\mathrm{D}_1\mathrm{q}_0-\eta_2q_0^2-2\mu\mathrm{D}_0\mathrm{q}_0-\eta_3\mathrm{q}_0^3 \tag{46}$$

Solution of Eq. (45) is obtained as follows

$$\mathrm{q}_0=\mathrm{A}(\mathrm{T}_1)\exp(\mathrm{i}\omega_0\mathrm{T}_0)+\Lambda\exp(\mathrm{i}\Omega\mathrm{T}_0)+\mathrm{CC} \tag{47}$$

where $\mathrm{A}(\mathrm{T}_1)$ is an unknown complex function and will be determined by eliminating the secular terms from $\mathbf{q_1}$, CC denotes the complex conjugated of the previous terms and $\boldsymbol{\Lambda}$ is a constant value and defined as follows

$$\Lambda=\frac{\mathrm{f}}{2}(\omega_0{}^2-\Omega^2)^{-1} \tag{48}$$

Substituting Eq. (47) into Eq. (46) yields

$$\begin{aligned}(\mathrm{D}_0^2+\omega_0^2)\mathrm{q}_1=&\begin{bmatrix}-2i\omega_0(D_1A+\mu A)\\-3\eta_3(A^2\bar{A}+2A\Lambda^2)\end{bmatrix}e^{i\omega_0T_0}\\&-\eta_2A^2e^{2i\omega_0T_0}-\eta_3\Lambda^3e^{3i\Omega T_0}-2\eta_2A\Lambda\begin{pmatrix}e^{iT_0(\Omega+\omega_0)}\\+e^{iT_0(\omega_0-\Omega)}\end{pmatrix}\\&-\eta_2\Lambda^2e^{2i\Omega T_0}-\eta_3A^3e^{3i\omega_0T_0}-\begin{bmatrix}3\eta_3(2A\bar{A}\Lambda+\Lambda^3)\\+2\mu i\Omega\Lambda\end{bmatrix}e^{i\Omega T_0}\\&-3\eta_3\mathrm{A}\Lambda^2\left[e^{iT_0(\omega_0+2\Omega)}+e^{iT_0(\omega_0-2\Omega)}\right]\\&-3\eta_3\bar{\mathrm{A}}^2\Lambda\left[e^{iT_0(\Omega-2\omega_0)}+e^{-iT_0(2\omega_0+\Omega)}\right]+CC\end{aligned} \tag{49}$$

Equating the source of secular terms in Eq. (49) to zero yields

$$\begin{aligned}-2i\omega_0(D_1A+\mu A)-2\eta_2A\Lambda(e^{i\Omega T_0}+e^{-i\Omega T_0})\\-3\eta_3(A^2\bar{A}+2A\Lambda^2)=0\end{aligned} \tag{50}$$

Considering $\mathrm{A}(\mathrm{T}_1)$ in the polar form as follows (Nayfeh *et al*. 1980):

$$A(T_1)=\frac{1}{2}a\,exp(i\beta) \tag{51}$$

where, a and β indicate real functions of T_1. Inserting Eq. (51) into Eq. (50) and separating the results in to its real and imaginary parts leads to

$$\acute{a}+\mu\mathrm{a}=0 \tag{52a}$$

$$a\acute{\beta}-\frac{3\eta_3}{\omega_0}\left(\frac{\alpha^3}{8}+\mathrm{a}\Lambda^2\right)=0 \tag{52b}$$

where, $(\acute{})$ is the first derivative with respect toT_1.Solving Eqs. (52a) and (52b) yields

$$a=\mathrm{a}_0e^{-\mu\epsilon\mathrm{t}} \tag{53a}$$

$$\beta=\frac{3\eta_3}{\omega_0}\left[\Lambda^2\boldsymbol{\epsilon t}-\frac{\mathrm{a}_0^2}{16\mu}e^{-2\mu\epsilon\mathrm{t}}\right]+\beta_0 \tag{53b}$$

where a_0 and $\beta_0$are constant of integration. Using of Eqs. (44), (47), (48) and (51) leads to

$$\begin{aligned}\mathrm{q}(\mathrm{t})=a\cos(\omega_0\mathrm{t}+\beta)+\mathrm{f}(\omega_0{}^2-\Omega^2)^{-1}\cos(\Omega\mathrm{t})\\+\mathrm{O}(\epsilon)\end{aligned} \tag{54}$$

In superharmonic resonance, the excitation frequency is near to one-third of the natural frequency of the system $\left(\Omega\approx\frac{1}{3}\omega_0\right)$. In such case to exhibit the nearness of Ω to ω_0 a detuning parameter, σ, is considered as below (Nayfeh *et al*. 1980):

$$3\Omega=\omega_0+\epsilon\sigma \tag{55}$$

Substituting Eq. (55) into Eq. (49) leads to

$$\begin{aligned}(\mathrm{D}_0^2+\omega_0^2)\mathrm{q}_1=&\begin{bmatrix}-2i\omega_0(D_1A+\mu A)\\-3\eta_3(A^2\bar{A}+2A\Lambda^2)-\eta_3\Lambda^3e^{i\sigma T_1}\end{bmatrix}e^{i\omega_0T_0}\\&-\eta_3A^3e^{3i\omega_0T_0}-2\eta_2A\Lambda\left(e^{iT_0(\Omega+\omega_0)}+e^{iT_0(\omega_0-\Omega)}\right)\\&-\eta_2A^2e^{2i\omega_0T_0}-\eta_2\Lambda^2e^{2i\Omega T_0}-\begin{bmatrix}3\eta_3(2A\bar{A}\Lambda+\Lambda^3)\\+2\mu i\Omega\Lambda\end{bmatrix}e^{i\Omega T_0}\\&-3\eta_3\mathrm{A}\Lambda^2\left[e^{iT_0(\omega_0+2\Omega)}+e^{iT_0(\omega_0-2\Omega)}\right]\\&-3\eta_3\mathrm{A}^2\Lambda\left[e^{iT_0(2\omega_0+\Omega)}+e^{iT_0(2\omega_0-\Omega)}\right]+CC\end{aligned} \tag{56}$$

To eliminate the secular terms in q_1, equating the coefficients of $\pm\exp(\mathrm{i}\omega_0\mathrm{T}_0)$ in Eq. (56) to zero as follows:

$$-2i\omega_0(D_1A+\mu A)3\eta_3(A^2\bar{A}+2A\Lambda^2)-\eta_3\Lambda^3e^{i\sigma T_1}=0 \quad (57)$$

Inserting Eq. (51) into Eq. (57) and then separating real and imaginary terms yields

$$\acute{a}+\mu a=-\frac{\eta_3\Lambda^3}{\omega_0}\sin\theta \quad (58a)$$

$$a(\sigma-\acute{\theta})-\frac{3\eta_3}{\omega_0}a\left[\frac{a^2}{8}+\Lambda^2\right]=\frac{\eta_3\Lambda^3}{\omega_0}\cos\theta \quad (58b)$$

where

$$\theta=\sigma T_1-\beta \quad (59)$$

In the case of steady state motion of the system the amplitude $\boldsymbol{a}$ and the phase of the system $\boldsymbol{\theta}$ are not charge at a singular point (Nayfeh *et al*. 1980):

$$\acute{a}=\acute{\theta}=0 \quad (60)$$

Substituting Eq. (60) into Eqs. (58a) and (58b) leads to:

$$\mu=-\frac{\eta_3\Lambda^3}{a\omega_0}\sin\theta \quad (61a)$$

$$\sigma-\frac{3\eta_3}{\omega_0}\left[\frac{a^2}{8}+\Lambda^2\right]=\frac{\eta_3\Lambda^3}{a\omega_0}\cos\theta \quad (61b)$$

Squaring and adding Eqs. (61a) and (61b) leads to the frequency response equation in superharmonic resonance as follows

$$\sigma=\frac{3\eta_3}{\omega_0}\left[\frac{a^2}{8}+\Lambda^2\right]\pm\sqrt{\frac{\eta_3^2\Lambda^6}{\omega_0^2a^2}-\mu^2} \quad (62)$$

Using of Eqs. (44), (47), (48), (51), (55), and (59), leads to the first approximation in superharmonic resonance as below

$$q=a\cos(3\Omega t-\theta)+f({\omega_0}^2-\Omega^2)^{-1}\cos(\Omega t)+O(\epsilon) \quad (63)$$

In the subharmonic resonance, the excitation frequency is close to three times of the natural frequency($\Omega\approx 3\omega_0$). In such case, the detuning parameter can be considered as below (Nayfeh *et al*. 1980):

$$\Omega=3\omega_0+\epsilon\sigma \quad (64)$$

Substituting Eq. (64) into Eq. (49) leads to

$$\begin{aligned}&(D_0^2+\omega_0^2)q_1\\&=\begin{bmatrix}-2i\omega_0(D_1A+\mu A)\\-3\eta_3(A^2\bar{A}+2A\Lambda^2)-3\eta_3\bar{A}^2\Lambda e^{i\sigma T_1}\end{bmatrix}e^{i\omega_0T_0}\\&-2\eta_2A\Lambda\left(e^{iT_0(\omega_0+\Omega)}+e^{iT_0(\omega_0-\Omega)}\right)-\eta_2\Lambda^2e^{2i\Omega T_0}\\&-\eta_2A^2e^{2i\omega_0T_0}-\eta_3A^3e^{3i\omega_0T_0}-\eta_3\Lambda^3e^{3i\Omega T_0}\\&-3\eta_3A\Lambda^2\left[e^{iT_0(\omega_0+2\Omega)}+e^{iT_0(\omega_0-2\Omega)}\right]\\&-3\eta_3\bar{A}^2\Lambda\left[e^{-iT_0(2\omega_0+\Omega)}\right]\\&-[3\eta_3(2A\bar{A}\Lambda+\Lambda^3)+2\mu i\Omega\Lambda]e^{i\Omega T_0}+CC\end{aligned} \quad (65)$$

Equating the source of secular terms in Eq. (65) to zero as follows

$$\begin{aligned}&2i\omega_0(D_1A+\mu A)+3\eta_3(A^2\bar{A}+2A\Lambda^2)\\&+3\eta_3\bar{A}^2\Lambda e^{i\sigma T_1}=0\end{aligned} \quad (66)$$

Substituting Eq. (51) into Eq. (66) and then separating real and imaginary terms yields

$$\acute{a}+\mu a=-\frac{3\eta_3\Lambda a^2}{4\omega_0}\sin\hat{\theta} \quad (67a)$$

$$a\left(\sigma-\hat{\acute{\theta}}\right)-\frac{9\eta_3}{\omega_0}a\left[\frac{a^2}{8}+\Lambda^2\right]=\frac{9\eta_3\Lambda a^2}{4\omega_0}\cos\hat{\theta} \quad (67b)$$

where

$$\hat{\theta}=\sigma T_1-3\beta \quad (68)$$

As mentioned before, in steady state motion, the amplitude $\boldsymbol{a}$ and the phase of the system $\widehat{\boldsymbol{\theta}}$ are not change in the singular point $\left(\acute{a}=\hat{\acute{\theta}}=0\right)$ (Nayfeh *et al*. 1980). Therefore, Eqs. (67a) and (67b) takes the following form

$$\mu a=-\frac{3\eta_3\Lambda a^2}{4\omega_0}\sin\hat{\theta} \quad (69a)$$

$$a(\sigma)-\frac{9\eta_3}{\omega_0}a\left[\frac{a^2}{8}+\Lambda^2\right]=\frac{9\eta_3\Lambda a^2}{4\omega_0}\cos\hat{\theta} \quad (69b)$$

Squaring and adding Eqs. (69a) and (69b) leads to the frequency response equation as follows:

$$\sigma=\frac{9\eta_3}{\omega_0}\left[\frac{a^2}{8}+\Lambda^2\right]\pm\sqrt{\frac{81\eta_3^2\Lambda^2a^2}{16\omega_0^2}-9\mu^2} \quad (70)$$

Using of Eqs. (44), (47), (48), (51), (64), and (68), leads to the first approximation in subharmonic resonance as below

$$q=a\cos\left[\frac{1}{3}(\Omega t-\hat{\theta})\right]+f({\omega_0}^2-\Omega^2)^{-1}\cos\Omega t+O(\epsilon) \quad (71)$$

where, Ω can be defined by using of Eqs. (64) and (70) as follows

$$\Omega=3\omega_0+\epsilon\left(\frac{9\eta_3}{\omega_0}\left[\frac{a^2}{8}+\Lambda^2\right]\pm\sqrt{\frac{81\eta_3^2\Lambda^2a^2}{16\omega_0^2}-9\mu^2}\right) \quad (72)$$

3. Findings and discussions

In numerical results, using material and geometry parameters are as follow (Wattanasakulpong and Ungbhakorn 2013, Yas and Samadi 2012): $E_{11}^{CNT}=600\,GPa$, $E_{22}^{CNT}=10\,GPa$, $G_{12}^{CNT}=17.2\,GPa$, $v^{CNT}=0.19$, $\rho^{CNT}=1400\,kg/m^3$, $E^p=2.5\,GPa$, $v^p=0.30$, and $\rho^p=1190\,kg/m^3$, L=300 μm; h=2 μm m, b=$2h$, length scale parameter(l) = 1.0 μm, amplitude of the load $f_0=0.015N$ maximum amplitude (Λ) = 1.0 μm.

In order to accuracy of present method, a comparison study is performed. For this purpose, the fundamental frequencies of a microscale simply supported beam made of pure polymer are calculated with different slenderness ratio and compared with those of Kong *et al*. (2008) corresponding to the Euler-Bernoulli beam theory in Table 2. In the obtaining of the vibration frequency from this study, the eigenvalue process is implemented in Eq. (38b).

Table 2 Comparative results for fundamental frequencies of a simply supported fully polymer microscale beam, $l = 0.5\ \mu$m.

$\frac{L}{h}$	Natural Frequency (MHz)	
	Kong *et al*. (2008)	Present
10.0	23.438	24.320
20.0	5.859	6.080
30.0	2.604	2.702
50.0	0.938	0.973
60.0	0.651	0.676
70.0	0.478	0.496
90.0	0.289	0.300
100.0	0.234	0.243

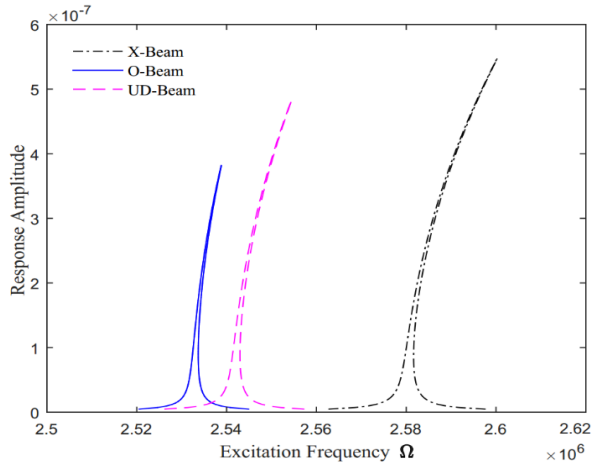

Fig. 2 The effect of different patterns of reinforcement on frequency responses in superharmonic resonance

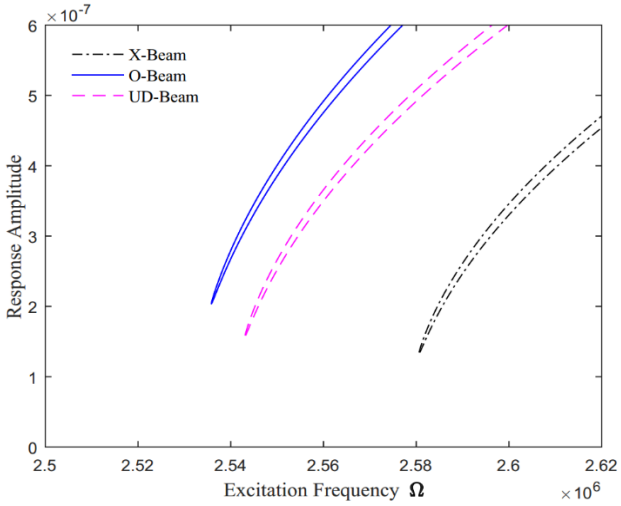

Fig. 3 The effect of different patterns of reinforcement on frequency responses in subharmonic resonance

It is found from Table 2, the current results are in good harmony with the related results of Ref. Kong *et al*. (2008). It is worth noting that, Kong *et al* (2008) neglected the contribution of the Poisson's which leads to the small difference between the results presented in Table 2.

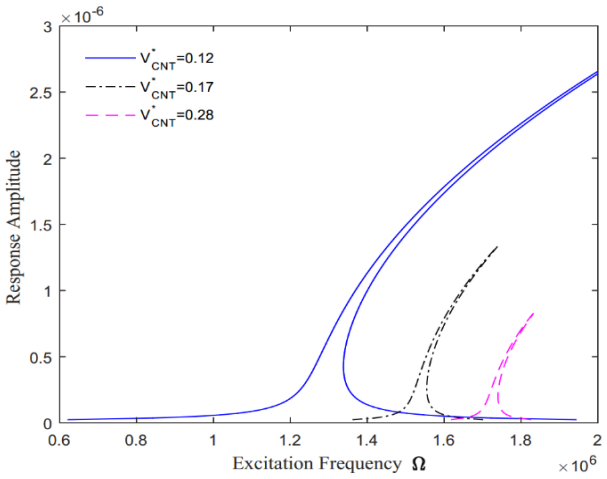

Fig. 4 The effect of V_{CNT}^{*} on frequency responses in superharmonic resonance for X distribution for $f_0 = 0.009\ N;\ C_d = 0.00006\ Pa.s, l = 9.0\mu m$

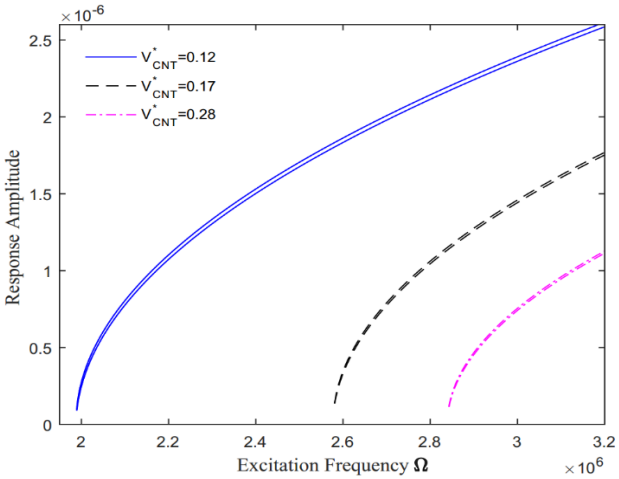

Fig. 5 The effect of V_{CNT}^{*} on frequency responses in subharmonic resonance for X distribution for $f_0 = 0.009\ N;\ C_d = 0.00006\ Pa.s,\ l = 17.6\mu m.$

Figs. 3 and 4 represent the effects of the pattern of reinforcement on the frequency response curves of the system in superharmonic and subharmonic resonance for $.V_{CNT}^{*} = 0.17;\ f_0 = 0.009\ N;\ C_d = 0.000003\ Pa.s, l = 17.6\mu m$, respectively. As shown in Figures 3 and 4, the frequency response curves consist of two branches. The upper branch represents the stable solution, the lower branch represents stable and unstable solutions. In subharmonic resonance, the lower branch represents the unstable solution. The deviation of the curves demonstrates the type of non-linearity. The curves deviated to the right which means that the system exhibits hardening type nonlinear behavior. As can be seen in Fig. 2, in superharmonic resonance, with changing the pattern of reinforcement in the order O, UD and X distrubutions, the hardening behavior of the system increase, the whole response region become wider and the height of the jump phenomena (sudden change in the amplitude and phase by small variation in the excitation frequency due to nonlinear nature of the system) increases. In addition, with changing the pattern of reinforcement in

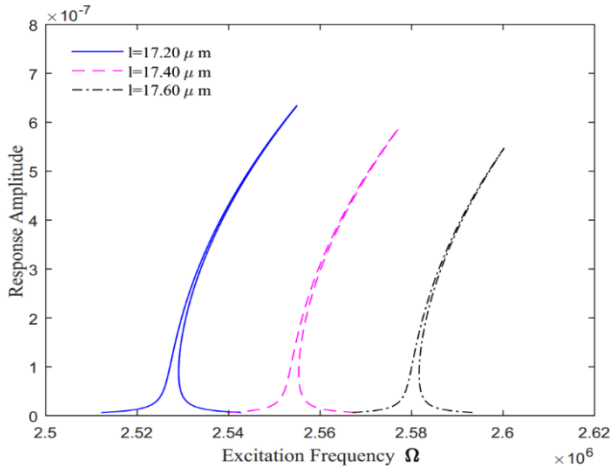

Fig. 6 The effect of material length scale parameter on frequency responses in superharmonic resonance for X distribution

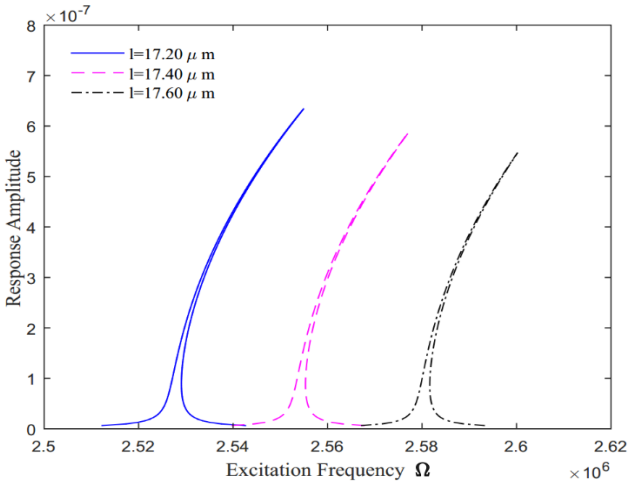

Fig. 8 The effect of forcing amplitude on frequency responses in superharmonic resonance for X distribution

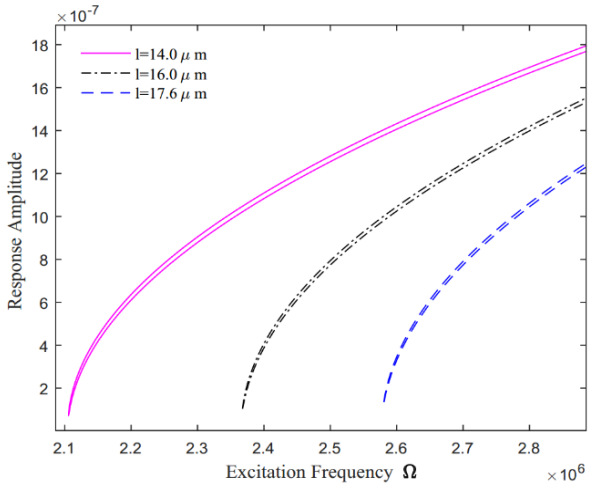

Fig. 7 The effect of material length scale parameter on frequency responses in subharmonic resonance for X distribution

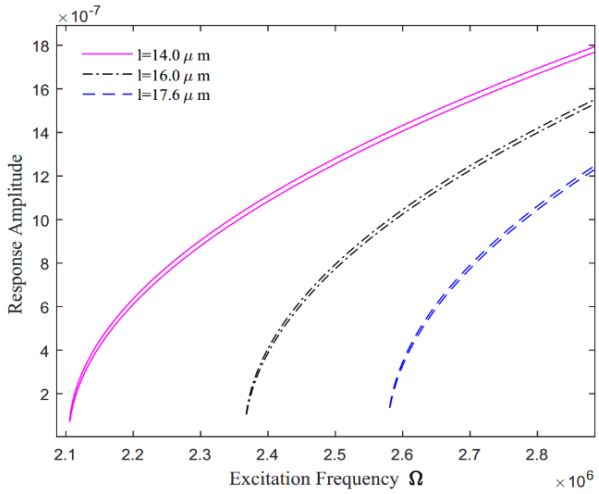

Fig. 9 The effect of forcing amplitude on frequency responses in subharmonic resonance for X distribution

the order O, UD and X, the peak amplitude of the nonlinear response and the nonlinear resonance frequency increases. Moreover, results show that, in Subharmonic resonance, with changing the pattern of reinforcement in the order O, UD and X, the minimum amplitude of the nonlinear response decreases. Furthermore, results illustrate that, for excitation frequencies in which Subharmonic resonance occur, the O has the lowest and the X has the highest.

In order to investigating the effects of the volume fraction V_{CNT}^{*} on the frequency responses in superharmonic and Subharmonic resonance Figs. 4 and 5 are presented for X distrubution, respectively. As can be seen in these figures, in superharmonic resonance, with increasing V_{CNT}^{*}, the whole response region become narrow, and the height of the jump phenomena and the peak amplitude of the nonlinear response decreases. Moreover, results demonstrated that, in subharmonic resonance with increasing V_{CNT}^{*}, the stable and unstable branches of the frequency responses got closer together and the subharmonic resonance occur at higher excitation frequency.

Figs. 6 and 7 represent the effects of the material length scale parameter on the frequency responses of the system in superharmonic and Subharmonic resonances for X distrubution for $f_0 = 0.009\,N;\ C_d = 0.000003\,Pa.$ respectively. Results of Figs. 6 and 7 show that, in superharmonic resonance with increasing the material length scale parameter, the peak amplitude of the nonlinear response decreases. However, the nonlinear resonance frequency increases. Moreover, the results demonstrate that in subharmonic resonance, with increasing the material length scale parameter the stable and unstable branches of the frequency responses get closer to gather, the minimum amplitude of the nonlinear response increases and the subharmonic resonance occur at higher excitation frequency.

In Figs. 8 and 9, the effects of the forcing amplitude on the frequency responses of the system for X distrubution for $C_d = 0.000003\ Pa.s,\ l = 17.6\,\mu m$ in superharmonic and subharmonic resonance, respectively. The presened results demonstrates that, the whole response region become wider, the height of the jump, the peak amplitude of the nonlinear

response and the nonlinear resonance frequency increases with increasing the forcing amplitude in superharmonic resonance. Moreover, as can be seen, in subharmonic resonance, the minimum amplitude of the nonlinear response increases, the stable and unstable solutions got closer together and the subharmonic resonance occur at higher excitation frequencies with increasing the forcing amplitude.

4. Conclusions

In this paper, superharmonic and subharmonic Resonances of a CNTRC microscale beam subjected to lateral harmonic load and damping force due to viscous medium are investigated based on modified couple stress theory. As reinforcing phase, three different types of CNTs distribution are considered. The governing nonlinear partial differential equation is derived based on the Euler-Bernoulli beam theory, von Kármán type of geometrical nonlinearity and Hamilton's principle. The Galerkin's decomposition technique is utilized to discretize the governing nonlinear partial differential equation to nonlinear ordinary differential equation and then is solved by using of multiple time scale method. The frequency response equation and the forced vibration response of the system are obtained. The effects of different patterns of reinforcement, the length scale parameter on the Frequency-Response Curves and phase trajectory of the Microscale carbon nanotube reinforced composite beam are investigated.

Through the numerical results, the most significant consequences are summarized as;

• The distribution of CNTs play an important role on superharmonic resonance. With changing the pattern of reinforcement in order; O, UD and X, the hardening behavior of the system increases. Moreover, excitation frequencies in which Subharmonic resonance occur, the O distribution has the lowest and the X distribution has the highest.

• V_{CNT}^{*} has important role on the nonlinear dynamic responses of the CNTRC beam. In superharmonic resonance increasing V_{CNT}^{*} yields to decreasing the peak amplitude of the nonlinear response. In addition, increasing V_{CNT}^{*} causes to the Subharmonic resonance occur at higher excitation frequency.

• Effects of the distribution and volume fraction of CNTs on the dynamic behavior significantly differ in superharmonic and subharmonic resonances.

• In superharmonic resonance with the increasing in the material length scale parameter, the peak amplitude of the nonlinear response decreases, however, the nonlinear resonance frequency increases. Moreover, the minimum amplitude of the nonlinear response increases and the subharmonic resonance occur at higher excitation frequency with the increasing in the material length scale parameter in subharmonic resonance.

• With the increasing in the amplitude of the excitation force, hardening behavior of the system remains steady in both superharmonic and subharmonic resonances, but the other responses differ significantly.

References

Akbaş, Ş.D. (2016a), "Forced vibration analysis of viscoelastic nanobeams embedded in an elastic medium", *Smart Struct. Syst.*, **18**(6), 1125-1143. https://doi.org/10.12989/sss.2016.18.6.1125.

Akbaş, Ş.D. (2016b), "Analytical solutions for static bending of edge cracked micro beams", *Struct. Eng. Mech.*, **59**(3),579-599. https://doi.org/10.12989/sem.2016.59.3.579.

Akbaş, Ş.D. (2016c), "Static analysis of a nano plate by using generalized differential quadrature method", *Int. J. Eng. Appl. Sci.*, **8**(2), 30-39. https://doi.org/10.24107/ijeas.252143.

Akbaş, Ş.D. (2017a), "Free vibration of edge cracked functionally graded microscale beams based on the modified couple stress theory", *Int. J. Struct. Stabil. Dyn.*, **17**(3),1750033. https://doi.org/10.1142/S021945541750033X.

Akbaş Ş.D. (2017b), *Static, Vibration, and Buckling Analysis of Nanobeams, Nanomechanics*, InTech, Rijeka, Croatia.

Akbaş, Ş.D. (2017c), "Forced vibration analysis of functionally graded nanobeams", *Int. J. Appl. Mech.*, **9**(7), 1750100. https://doi.org/10.1142/S1758825117501009.

Akbaş, Ş.D. (2018a), "Forced vibration analysis of cracked functionally graded microbeams", *Adv. Nano Res.*, **6**(1), 39-55. https://doi.org/10.12989/anr.2018.6.1.039.

Akbaş, Ş.D. (2018b), "Forced vibration analysis of cracked nanobeams", *J. Brazil. Soc. Mech. Sci. Eng.*, **40**(8), 392. https://doi.org/10.1007/s40430-018-1315-1.

Akbaş, Ş.D. (2018c), "Bending of a cracked functionally graded nanobeam", *Adv. Nano Res.*, **6**(3), 219-242. https://doi.org/10.12989/anr.2018.6.3.219.

Akbaş, Ş.D. (2019a) "Axially forced vibration analysis of cracked a nanorod", *J. Comput. Appl. Mech.*, **5**(2), 477-485. https://doi.org/10.22059/JCAMECH.2019.281285.392.

Akbaş, Ş.D. (2019b) "Longitudinal forced vibration analysis of porous a nanorod", *Mühendislik Bilimleri ve Tasarım Dergisi*, **7**(4), 736-743. https://doi.org/10.21923/jesd.553328.

Al-Furjan, M.S.H., Habibi, M., Won Jung, D., Sadeghi, S., Safarpour, H., Tounsi, A. and Chen, G. (2020), "A computational framework for propagated waves in a sandwich doubly curved nanocomposite panel", *Eng. Comput.*, 1-18. https://doi.org/10.1007/s00366-020-01130-8.

Alimoradzadeh, M., Salehi, M. and Esfarjani, S.M. (2019), "Nonlinear dynamic response of an axially functionally graded (AFG) beam resting on nonlinear elastic foundation subjected to moving load", *Nonlinear Eng.*, **8**(1), 250-260. https://doi.org/10.1515/nleng-2018-0051.

Alimoradzadeh, M., Salehi, M. and Esfarjani, S.M. (2020), "Nonlinear vibration analysis of axially functionally graded microbeams based on nonlinear elastic foundation using modified couple stress theory", *Period. Polytech. Mech. Eng.*, **64**(2), 97-108. https://doi.org/10.3311/PPme.11684.

Alimoradzadeh, M. and Akbaş, Ş.D. (2021) "Superharmonic and subharmonic resonances of atomic force microscope subjected to crack failure mode based on the modified couple stress theory", *Eur. Phys. J. Plus*, **136**(5), 1-20. https://doi.org/10.1140/epjp/s13360-021-01539-0.

Ansari, M., Esmailzadeh, E. and Younesian, D. (2010), "Internal-external resonance of beams on non-linear viscoelastic foundation traversed by moving load", *Nonlinear Dynam.*, **61**(1), 163-182. https://doi.org/10.1007/s11071-009-9639-0.

Babu Arumugam, A., Rajamohan, V., Bandaru, N., Sudhagar P.E. and Kumbhar, S.G. (2019), "Vibration analysis of a carbon nanotube reinforced uniform and tapered composite beams", *Arch. Acoust.*, **44**(02), 309-320. http://doi.org/10.24425/aoa.2019.128494.

Bousahla, A.A., Bourada, F., Mahmoud, S.R., Tounsi, A., Algarni, A., Bedia, E.A. and Tounsi, A. (2020), "Buckling and dynamic

behavior of the simply supported CNT-RC beams using an integral-first shear deformation theory", *Comput. Concrete*, **25**(2), 155-166. https://doi.org/10.12989/cac.2020.25.2.155.

Civalek, Ö., Dastjerdi, S., Akbaş, Ş.D. and Akgöz, B. (2021a) "Vibration analysis of carbon nanotube-reinforced composite microbeams", *Math. Method Appl. Sci*., Special Issue Paper. https://doi.org/10.1002/mma.7069.

Civalek, Ö., Akbaş, Ş.D., Akgöz, B. and Dastjerdi, S. (2021b), "Forced vibration analysis of composite beams reinforced by carbon nanotubes", *Nanomaterials*, **11**(3), 571. https://doi.org/10.3390/nano11030571.

Chu, H., Li, Y., Wang, C., Zhang, H., Li, D. (2020), "Recent investigations on nonlinear absorption properties of carbon nanotubes", *Nanophotonics*, **9**(4), 761-781. https://doi.org/10.1515/nanoph-2020-0085.

Ebrahimi F., Shaghaghi G.R., Boreiry M., (2016), "An investigation into the influence of thermal loading and surface effects on mechanical characteristics of nanotubes", *Struct. Eng. Mech*., **57**(1), 179-200. http://doi.org/10.12989/sem.2016.57.1.179.

Ebrahimi, F. and Dabbagh, A. (2018a), "Wave propagation analysis of magnetostrictive sandwich composite nanoplates via nonlocal strain gradient theory", *Proceedings of the Institution of Mechanical Engineers, Part C: Journal of Mechanical Engineering Science*, **232**(22), 4180-4192. https://doi.org/10.1177/0954406217748687.

Ebrahimi, F. and Dabbagh, A. (2018b), "Wave dispersion characteristics of embedded graphene platelets-reinforced composite microplates", *Eur. Phys. J. Plus*, **133**(4), 1-13. https://doi.org/10.1140/epjp/i2018-11956-5.

Ebrahimi, F. and Dabbagh, A. (2018c), "On wave dispersion characteristics of double-layered graphene sheets in thermal environments", *J. Electromagnetic Wave Appl*., **32**(15), 1869-1888. https://doi.org/10.1080/09205071.2017.1417918.

Fernandes, R., Mousavi, S. M. and El-Borgi, S. (2016), "Free and forced vibration nonlinear analysis of a microbeam using finite strain and velocity gradients theory", *Acta Mech*., **227**(9), 2657-2670. https://doi.org/10.1007/s00707-016-1646-x.

Ghayesh, M.H. (2009), "Stability characteristics of an axially accelerating string supported by an elastic foundation", *Mech. Mach Theory*, **44**(10), 1964-1979. https://doi.org/10.1016/j.mechmachtheory.2009.05.004.

Ghayesh, M.H. (2012), "Nonlinear dynamic response of a simply-supported Kelvin–Voigt viscoelastic beam, additionally supported by a nonlinear spring", *Nonlinear Anal. Appl*., **13**(3), 1319-1333. https://doi.org/10.1016/j.nonrwa.2011.10.009.

Ghayesh, M.H., Amabili, M. and Païdoussis, M.P. (2012a), "Thermo-mechanical phase-shift determination in Coriolis mass-flowmeters with added masses", *J. Fluid Struct*., **34**, 1-13. https://doi.org/10.1016/j.jfluidstructs.2012.05.003.

Ghayesh, M.H., Kazemirad, S. and Reid, T. (2012b), "Nonlinear vibrations and stability of parametrically exited systems with cubic nonlinearities and internal boundary conditions: A general solution procedure", *Appl. Math. Modell*., **36**(7), 3299-3311. https://doi.org/10.1016/j.apm.2011.09.084.

Ghayesh, M.H. (2018a), "Nonlinear vibrations of axially functionally graded Timoshenko tapered beams", *J. Comput. Nonlinear Dyn*., **13**(4), 041002. https://doi.org/10.1115/1.4039191.

Ghayesh, M.H. (2018b), "Nonlinear dynamics of multilayered microplates", *J. Comput. Nonlinear Dyn*., **13**(2), 021006. https://doi.org/10.1115/1.4037596.

Guo, X.Y. and Zhang, W. (2016), "Nonlinear vibrations of a reinforced composite plate with carbon nanotubes", *Compos. Struct*., **135**, 96-108. https://doi.org/10.1016/j.compstruct.2015.08.063.

Heidari, M. and Arvin, H. (2019), "Nonlinear free vibration analysis of functionally graded rotating composite Timoshenko beams reinforced by carbon nanotubes", *J. Vib. Control*, **25**(14), 2063-2078. http://doi.org/10.1016/j.compstruct.2016.12.009.

Huang, Y., Karami, B., Shahsavari, D. and Tounsi, A. (2021), "Static stability analysis of carbon nanotube reinforced polymeric composite doubly curved micro-shell panels", *Arch. Civil Mech. Eng*., **21**(4), 1-15. https://doi.org/10.1007/s43452-021-00291-7.

Iijima, S. (1991), "Helical microtubules of graphitic carbon", *Nature*, **354**(56-58), 56-58. http://doi.org/10.1038/354056a0.

Ke, L.L., Yang, J. and Kitipornchai, S. (2010), "Nonlinear free vibration of functionally graded carbon nanotube-reinforced composite beams", *Compos. Struct*., **92**(3), 676-683. https://doi.org/10.1016/j.compstruct.2009.09.024.

Kocatürk, T. and Akbaş, Ş.D. (2013), "Wave propagation in a microbeam based on the modified couple stress theory", *Struct. Eng. Mech*., **46**(3), 417-431. https://doi.org/10.12989/sem.2013.46.3.417.

Kong, S., Zhou, S., Nie, Z. and Wang, K. (2008), "The size-dependent natural frequency of Bernoulli–Euler micro-beams", *Int. J. Eng. Sci*., **46**(5), 427-437. https://doi.org/10.1016/j.ijengsci.2007.10.002.

Kumar, Y., Gupta, A. and Tounsi, A. (2021), "Size-dependent vibration response of porous graded nanostructure with FEM and nonlocal continuum model", *Adv. Nano Res*., **11**(1), 1-17. https://doi.org/10.12989/anr.2021.11.1.001.

Li, Y.H., Wei, J., Zhang, X., Xu, C., Wu, D., Lu, L. and Wei, B. (2002), "Mechanical and electrical properties of carbon nanotube ribbons", *Chem. Phys. Lett*., **365**(1-2), 95-100. https://doi.org/10.1016/S0009-2614(02)01434-3.

Mamidi, N., Leija, H. M., Diabb, J.M., Lopez Romo, I., Hernandez, D., Castrejón, J.V., Romero, O.M., Barrera, E.V. and Zúñiga, A.E. (2017), "C ytotoxicity evaluation of unfunctionalized multiwall carbon nanotubes-ultrahigh molecular weight polyethylene nanocomposites", *J. Biomed. Mater. Res. A*, **105**(11), 3042-3049. https://doi.org/10.1002/jbm.a.36168.

Mamidi, N. (2019), "Cytotoxicity evaluation of carbon nanotubes for biomedical and tissue engineering applications", *Perspect. Carbon Nanotub*, **12**. https://doi.org/10.5772/intechopen.85899.

Mamidi, N., Delgadillo, R.M.V. and Castrejón, J.V. (2021), "Unconventional and facile production of stimuli-responsive multifunctional system for simultaneous drug delivery and environmental remediation", *Environ. Sci. Nano*, **8**(7), 2081-2097. https://doi.org/10.1039/D1EN00354B.

Nayfeh, A.H., Mook, D.T. and Holmes, P. (1980), "Nonlinear oscillations", *ASME. J. Appl. Mech*, **47**(3), 692. https://doi.org/10.1115/1.3153771.

Ponnusami, S.A., Gupta, M. and Harursampath, D. (2019), "Asymptotic modeling of nonlinear bending and buckling behavior of carbon nanotubes", *AIAA J*., **57**(10), 4132-4140. https://doi.org/10.2514/1.J057564.

Rafiee, M., He, X.Q. and Liew, K.M. (2014), "Non-linear dynamic stability of piezoelectric functionally graded carbon nanotube-reinforced composite plates with initial geometric imperfection", *Int. J. Non-Linear Mech*., **59**, 37-51. https://doi.org/10.1016/j.ijnonlinmec.2013.10.011

Rao, S.S. (2007), *Vibration of Continuous Systems*, Wiley, New York, U.S.A.

Ruoff, R.S. and Lorents, D.C. (1995), "Mechanical and thermal properties of carbon nanotubes", *Carbon*, **33**(7), 925-930. https://doi.org/10.1016/0008-6223(95)00021-5.

Salvetat, J.P., Bonard, J.M., Thomson, N.H., Kulik, A.J., Forro, L., Benoit, W. and Zuppiroli, L. (1999), "Mechanical properties of carbon nanotubes", *Appl. Phys. A*, **69**(3), 255-260. https://doi.org/10.1007/s003390050999.

Shafiei, H. and Setoodeh, A.R. (2017), "Nonlinear free vibration and post-buckling of FG-CNTRC beams on nonlinear

foundation", *Steel Compos. Struct.*, **24**(1), 65-77. http://doi.org/10.12989/scs.2017.24.1.065.

Shen, H.S. (2009), "Nonlinear bending of functionally graded carbon nanotube-reinforced composite plates in thermal environments", *Compos. Struct.*, **91**(1), 9-19. https://doi.org/10.1016/j.compstruct.2009.04.026.

Shi, Z., Yao, X., Pang, F. and Wang, Q. (2017), "An exact solution for the free-vibration analysis of functionally graded carbon-nanotube-reinforced composite beams with arbitrary boundary conditions", *Sci. Rep.*, **7**(1), 1-18. https://doi.org/10.1038/s41598-017-12596-w.

Şimşek, M. (2014), "Nonlinear static and free vibration analysis of microbeams based on the nonlinear elastic foundation using modified couple stress theory and He's variational method", *Compos. Struct.*, **112**, 264-272. https://doi.org/10.1016/j.compstruct.2014.02.010.

Tagrara, S.H., Benachour, A, Bouiadjra M.B., Tounsi, A. (2015), "On bending, buckling and vibration responses of functionally graded carbon nanotube-reinforced composite beams", *Steel Compos. Struct.*, **19**(5), 1259-1277. http://doi.org/10.12989/scs.2015.19.5.1259.

Thang, P.T., Nguyen, T.T. and Lee, J. (2017), "A new approach for nonlinear buckling analysis of imperfect functionally graded carbon nanotube-reinforced composite plates", *Compos. Part B Eng.*, **127**, 166-174. http://doi.org/10.1016/j.compositesb.2016.12.002.

Ton-That, H.L. (2020), "The linear and nonlinear bending analyses of functionally graded carbon nanotube-reinforced composite plates based on the novel four-node quadrilateral element", *Eur. J. Comput. Mech.*, 139-172. https://doi.org/10.13052/ejcm2642-2085.2915.

Tornabene, F., Bacciocchi, M., Fantuzzi, N. and Reddy, J.N. (2019), "Multiscale approach for three-phase CNT/polymer/ fiber laminated nanocomposite structures", *Polym. Compos.*, **40**(S1), 102-126. https://doi.org/10.1002/pc.24520.

Van Do, V.N., Jeon, J.T. and Lee, C.H. (2020), "Dynamic analysis of carbon nanotube reinforced composite plates by using Bézier extraction based isogeometric finite element combined with higher-order shear deformation theory", *Mech. Mater.*, **142**, 103307. http://doi.org/10.1016/j.mechmat.2019.103307.

Wattanasakulpong, N. and Ungbhakorn, V. (2013), "Analytical solutions for bending, buckling and vibration responses of carbon nanotube-reinforced composite beams resting on elastic foundation", *Comput. Mater. Sci.*, **71**, 201-208. http://doi.org/10.1016/j.commatsci.2013.01.028.

Wu, C.P., Chen, Y.H., Hong, Z.L. and Lin, C.H. (2018), "Nonlinear vibration analysis of an embedded multi-walled carbon nanotube", *Adv. Nano Res.*, **6**(2), 163-182. https://doi.org/10.12989/anr.2018.6.2.163.

Yakobson, B.I. and Avouris, P. (2001), "Mechanical properties of carbon nanotubes", *Carbon Nanotub.*, 287-327. https://doi.org/10.1007/3-540-39947-X_12.

Yas, M.H. and Samadi, N. (2012), "Free vibrations and buckling analysis of carbon nanotube-reinforced composite Timoshenko beams on elastic foundation", *Int. J. Pres. Ves. Pip.*, **98**, 119-128. https://doi.org/10.1016/j.ijpvp.2012.07.012.

Zavala, J.M.D., Gutiérrez, H.M.L., Segura-Cárdenas, E., Mamidi, N., Morales-Avalos, R., Villela-Castrejón, J. and Elías-Zúñiga, A. (2021), "Manufacture and mechanical properties of knee implants using SWCNTs/UHMWPE composites", *J. Mech. Behav. Biomed. Mater.*, **120**, 104554. https://doi.org/10.1016/j.jmbbm.2021.104554.